

Perspective

Fiber-Optic Based Laser Wakefield Accelerated Electron Beams and Potential Applications in Radiotherapy Cancer Treatments

Dante Roa ^{1,*}, Jeffrey Kuo ¹, Harry Moyses ¹, Peter Taborek ², Toshiki Tajima ², Gerard Mourou ³ and Fuyuhiko Tamanoi ^{4,5} 

¹ Department of Radiation Oncology, Chao Family Comprehensive Cancer Center, University of California, Irvine-Medical Center, 101 The City Drive, B-23, Orange, CA 92868, USA; jvkuo@hs.uci.edu (J.K.); mikemoyses@hotmail.com (H.M.)

² Department of Physics and Astronomy, University of California, Irvine, CA 92697, USA; ptaborek@uci.edu (P.T.); ttajima@uci.edu (T.T.)

³ Ecole Polytechnique, 91128 Paliseau, France; gerard.mourou@polytechnique.edu

⁴ Institute for Integrated Cell-Materials Science, Institute for Advanced Study, Kyoto University, Kyoto 606-8501, Japan; tamanoi.fuyuhiko.2c@kyoto-u.ac.jp

⁵ Department of Microbiology, Immunology and Molecular Genetics, University of California, Los Angeles, CA 90095, USA

* Correspondence: droa@hs.uci.edu

Abstract: Ultra-compact electron beam technology based on laser wakefield acceleration (LWFA) could have a significant impact on radiotherapy treatments. Recent developments in LWFA high-density regime (HD-LWFA) and low-intensity fiber optically transmitted laser beams could allow for cancer treatments with electron beams from a miniature electronic source. Moreover, an electron beam emitted from a tip of a fiber optic channel could lead to new endoscopy-based radiotherapy, which is not currently available. Low-energy (10 keV–1 MeV) LWFA electron beams can be produced by irradiating high-density nano-materials with a low-intensity laser in the range of $\sim 10^{14}$ W/cm². This energy range could be useful in radiotherapy and, specifically, brachytherapy for treating superficial, interstitial, intravascular, and intracavitary tumors. Furthermore, it could unveil the next generation of high-dose-rate brachytherapy systems that are not dependent on radioactive sources, do not require specially designed radiation-shielded rooms for treatment, could be portable, could provide a selection of treatment energies, and would significantly reduce operating costs to a radiation oncology clinic.

Keywords: LWFA; fiber optics; medicine; brachytherapy; cancer



Citation: Roa, D.; Kuo, J.; Moyses, H.; Taborek, P.; Tajima, T.; Mourou, G.; Tamanoi, F. Fiber-Optic Based Laser Wakefield Accelerated Electron Beams and Potential Applications in Radiotherapy Cancer Treatments. *Photonics* **2022**, *9*, 403. <https://doi.org/10.3390/photonics9060403>

Received: 26 March 2022

Accepted: 6 June 2022

Published: 8 June 2022

Publisher's Note: MDPI stays neutral with regard to jurisdictional claims in published maps and institutional affiliations.



Copyright: © 2022 by the authors. Licensee MDPI, Basel, Switzerland. This article is an open access article distributed under the terms and conditions of the Creative Commons Attribution (CC BY) license (<https://creativecommons.org/licenses/by/4.0/>).

1. Introduction

Laser wakefield acceleration (LWFA) was initially proposed by Tajima and Dawson in 1979 as a method to accelerate charged particles from a low-density plasma using wave-like oscillations induced by electromagnetic pulses from a laser beam targeting the plasma [1]. They calculated that a high-intensity laser of 1 μm wavelength and 10^{18} W/cm² of power irradiating a plasma density of 10^{18} cm⁻³ could accelerate electrons to GeV energies over a 1 cm distance.

Experimental verification of LWFA came to light with the advent of high-intensity short-pulse lasers (e.g., Nd: glass laser; 10^{17} – 10^{18} W cm⁻²; 1 ps pulse width) and chirped pulse amplification (CPA) technology described by Strickland and Mourou in 1985 [2]. Soon after, several groups reported electron accelerations to energies in the MeV to GeV range [3,4]. However, the electron beam current, attributed to pulse repetition rate, was significantly lower compared to conventional linear accelerators (linacs), and beam quality, reproducibility, and stability were not consistent in most cases [4].

Subsequent experiments demonstrated the production of monoenergetic electron beams of 25–170 MeV energies [5–9] using compact laser-plasma acceleration systems,

which ignited the interest in a potential replacement of radiotherapy linacs with this technology. Since then, the use of LWFA in radiotherapy has focused on the production of external and clinically useful high-energy X-ray, electron [10–13], and proton [13–17] beams, but to date, there is still no commercially available device with this technology.

Conversely, limited attention has been devoted to the production of low-energy LWFA electron beams in the keV to MeV range. Production of these beams can be achieved by increasing the plasma density, thereby reducing the electron energy gain. Furthermore, the technology can be compact. Therefore, an LWFA electron beam could be produced from the tip of micron thick flexible fiber-optic channel that could transport a laser beam, as demonstrated by Nicks et al. [18] and, in a companion paper, by Barraza-Valdez et al. [19].

This could have a significant impact in radiation therapy and especially brachytherapy, which is a cancer treatment technique that delivers a high radiation dose in close proximity (≤ 1 cm) and/or inside a tumor volume in a patient's body [20,21].

This paper provides an overview of the production, medical applications, benefits, and cost reduction that an LWFA electron beam emitted from thin and flexible fiber-optic channels could have in radiotherapy.

2. Rationale

The interaction of a laser beam with plasma resembles that of a tsunami wave traveling through a body of water. If the tsunami travels in deep waters, its phase velocity can be very fast, and very few elements can get trapped and accelerated to these velocities. Likewise, when a laser interacts with a low-density plasma, the laser wake phase velocity can approach the speed of light, and a few electrons are captured by the laser wake and accelerated to very high energies.

On the other hand, if the tsunami travels in shallow waters, its phase velocity is very slow, but its amplitude is very high, trapping a significant amount of sediment in the process. Similarly, when a laser interacts with a high-density plasma, its phase velocity is significantly reduced ($v_g \sim 0$), and a strong coupling of the laser to the plasma motion occurs. In essence, this is what occurs in the production of low-energy LWFA electrons.

In these interactions, the LWFA electron energy gain changes from a relativistic (Tajima-Dawson [1]) to a non-relativistic interaction, as described by Barraza-Valdez et al. [19], with a sharp reduction of maximum electron energy as a function of the normalized laser intensity, a_0 , which in this case approaches unity, as demonstrated by Nicks et al. [18]. Moreover, the ratio of the laser critical density, n_c , and the plasma density, n_e , also approaches unity at a given a_0 , resulting in excited and broad plasma waves [19], and with virtually complete absorption and/or conversion of the laser energy to an electron beam energy.

The combination of multiple plasma waves produces consecutive electron trappings (and thus acceleration) over a wider range of plasma waves. This allows for occasional electron energy increases when the electron density increases, as opposed to the standard laser wakefield theory scaling described by Tajima and Dawson [1]. Increasing the laser pulse length leads to more electrons accelerated which yields a larger dose deposition, as shown in Figure 1.

For this application, the electron beam is produced by a laser beam traveling through a fiber optic channel until it reaches a lens located near the tip of the channel. The lens compresses the laser pulse and directs it to a micron-sized cavity filled with nano-tube fabric near critical density. The electrons in the cavity are separated by the electromagnetic field induced by the laser and accelerated to keV–MeV energies through LWFA, which produces the electron beam to be used for treatment (Figure 2).

Theoretical and computational studies by Barraza-Valdez et al. [19] have demonstrated that the proposed laser-matter interactions, with laser intensities of $\sim 10^{14}$ W/cm² and 10–100 micron target(s) at critical density, can yield a 10 keV electron beam via LWFA. Furthermore, Sha et al. [22] have described that fiber laser technology for this regime is feasible.

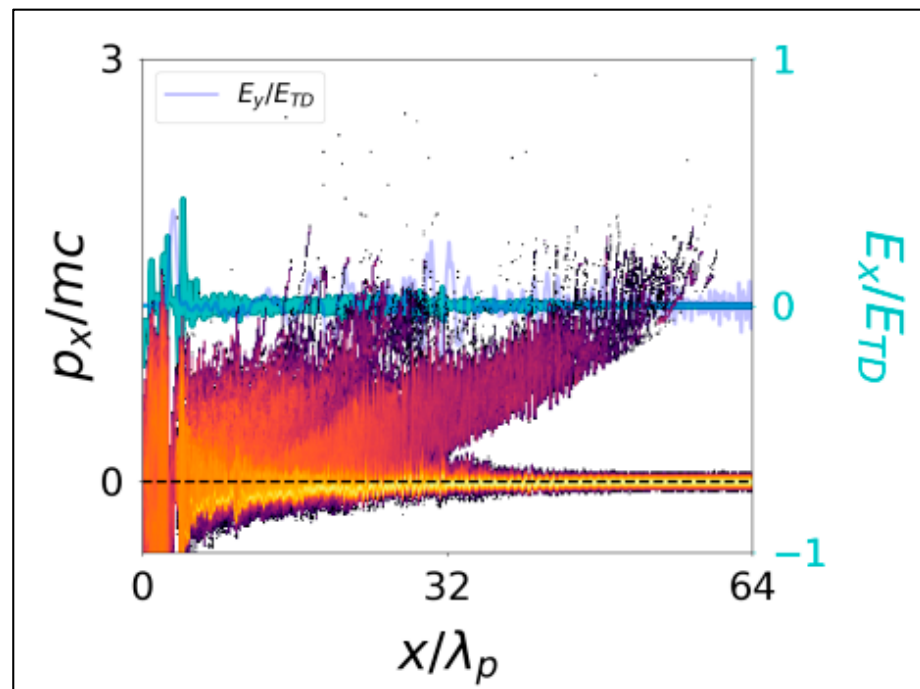


Figure 1. Electron phase space and field structure for a critical density case $n_c/n_e = 1$ and a laser pulse of length $8\lambda_p$ at a laser intensity $a_0 = 1$. Data shows the buildup of a large population of low-energy accelerated electrons for a high-density plasma (from Nicks et al. [18]).

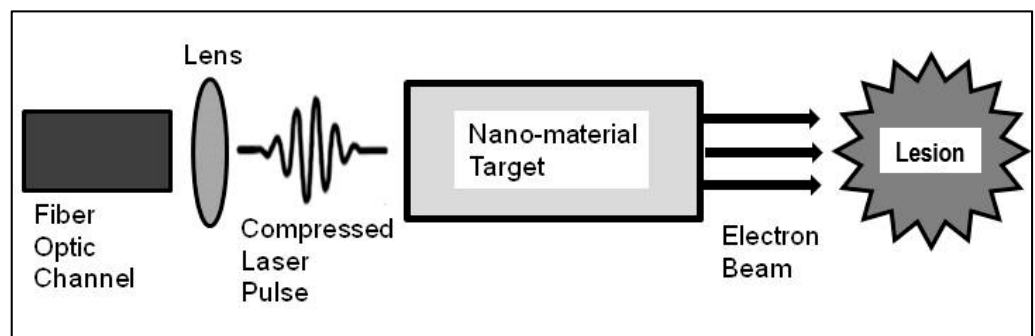


Figure 2. Schematic of a fiber optic channel and laser beam traveling through the fiber. At the end of the fiber, the laser enters a micro-lens which compresses the laser pulse prior to entering a high-density nano-tube fabric target. The target is near its critical density materials, which is the result of a nano-tube fabric spanned from a set of struts. An electron beam, produced from the LWFA interaction of the laser with a high-density target, is used for treatment. It is envisioned that the fiber optic channel, lens, and target cavity setup to be in the ~ 100 micron scale, and the electron beam could be aimed directly at a lesion volume.

3. Significance

3.1. Applications to Brachytherapy

Brachytherapy is a radiotherapy technique that delivers a large radiation dose adjacent to or inside a tumor in a patient’s body [20,21]. The dose is delivered in one or more sessions and effectively conforms to the tumor volume due to its treatment proximity while minimizing collateral radiation dose to healthy organs nearby [21]. Superficial, intracavitary, interstitial, intravascular, and endoscopic brachytherapy techniques are available for treatment. Interstitial brachytherapy may require the patient to stay in the hospital overnight, while the others, for the most part, are outpatient procedures [21].

Gamma-emitting sources (e.g., ^{226}Ra , ^{137}Cs , ^{60}Co , ^{198}Au , ^{192}Ir , ^{103}Pd , and ^{131}Cs) with energies ranging from 0.2–0.8 MeV have been used for decades in needles, seeds, and

ribbons for gynecological and prostate brachytherapy [23]. Further, electron-emitting sources (e.g., ^{90}Y , 0.9–2.3 MeV) in the form of microspheres are used in solutions to treat intrahepatic cancers [24–28].

Currently, high-dose-rate (HDR) brachytherapy units equipped with either a 10 Curie (Ci) ^{192}Ir (half-life of 73.8 days) or a 2.4 Ci ^{60}Co (half-life of 5.3 years) gamma-ray source inside a capsule, the size of a grain of rice and welded to the tip of a flexible wire, are routinely used in brachytherapy [23,28–30]. Even though kilovoltage X-rays from electronic generators have become available [31], HDR brachytherapy with gamma-ray sources remains the prevalent treatment modality.

HDR brachytherapy can deliver effective superficial, intracavitary, and interstitial treatments. However, source decay that leads to progressively longer treatment times, source replacement costs, and shielding costs are major drawbacks. For instance, an interstitial gynecological brachytherapy treatment with 20 implanted hollow needles treating a patient's cervix to a dose of 6 Gy in one fraction could take 5 min. (300 s) treatment time with a new (10 Ci) ^{192}Ir source (3000 Ci \times seconds). A similar treatment (3000 Ci \times seconds) delivered 4 months later (\sim 3 Ci) would take 17 min. treatment time.

An HDR system based on LWFA (LWFA-HDR) could eliminate these disadvantages by removing the radioactive source and, instead, produce electron beams that can be easily shielded. Furthermore, it could eliminate the threat of stolen radioactive material that could be used as a dirty bomb, as stated by the United States Department of Homeland Security, and eliminate radiation safety accidents due to damage and/or mishandling of a radioactive source [32]. Further, radiation oncology clinics in the United States would not be bound by the Nuclear Regulatory Commission (NRC) for HDR clinical operations since a radioactive source would not be needed.

3.2. Current HDR and Potential LWFA-HDR Treatment

Delivery of an HDR brachytherapy treatment consists of sending a radioactive source attached to the tip of a flexible wire through a catheter connected to a brachytherapy applicator inside or adjacent to a tumor (lesion) volume. Some examples of brachytherapy applicators include surface applicators for skin cancer treatments (Figure 3a), cylindrical applicators of different diameters for vaginal or rectal treatments (Figure 3b), tandem-and-ovoids applicators for cervical and uterine treatments (Figure 3c), and hollow needles for interstitial treatments (e.g., gynecological and prostate) (Figure 3d).

Each applicator has a channel where the source stops at multiple predetermined locations for specific times to deliver a portion of the prescribed radiation dose. These locations are known as dwell positions and the times as dwell times (Figure 3e). An applicator may have more than one insertion channel, each connected to a corresponding catheter and with specific dwell positions/times per channel. Figure 3f-top shows 7 out of 8 catheters of a SAVI breast applicator (Cianna Medical, Aliso Viejo, CA, USA) connected to an HDR unit. Figure 3f-bottom shows a coronal radiograph of the SAVI applicator inside a patient. This applicator is inserted in a breast cavity left after surgical removal of a tumor (lumpectomy). Brachytherapy treatment is administered to eliminate any residual microscopic malignancies.

A computer simulation of the brachytherapy treatment delivery is performed before a patient receives their treatment. For this purpose, a computer tomography (CT) scan, encompassing the treatment region and the brachytherapy applicator, is used in the simulation to determine the dwell positions and dwell times needed to achieve a conformal radiation dose distribution around the tumor volume (Figure 4) while minimizing dose to nearby healthy organs.

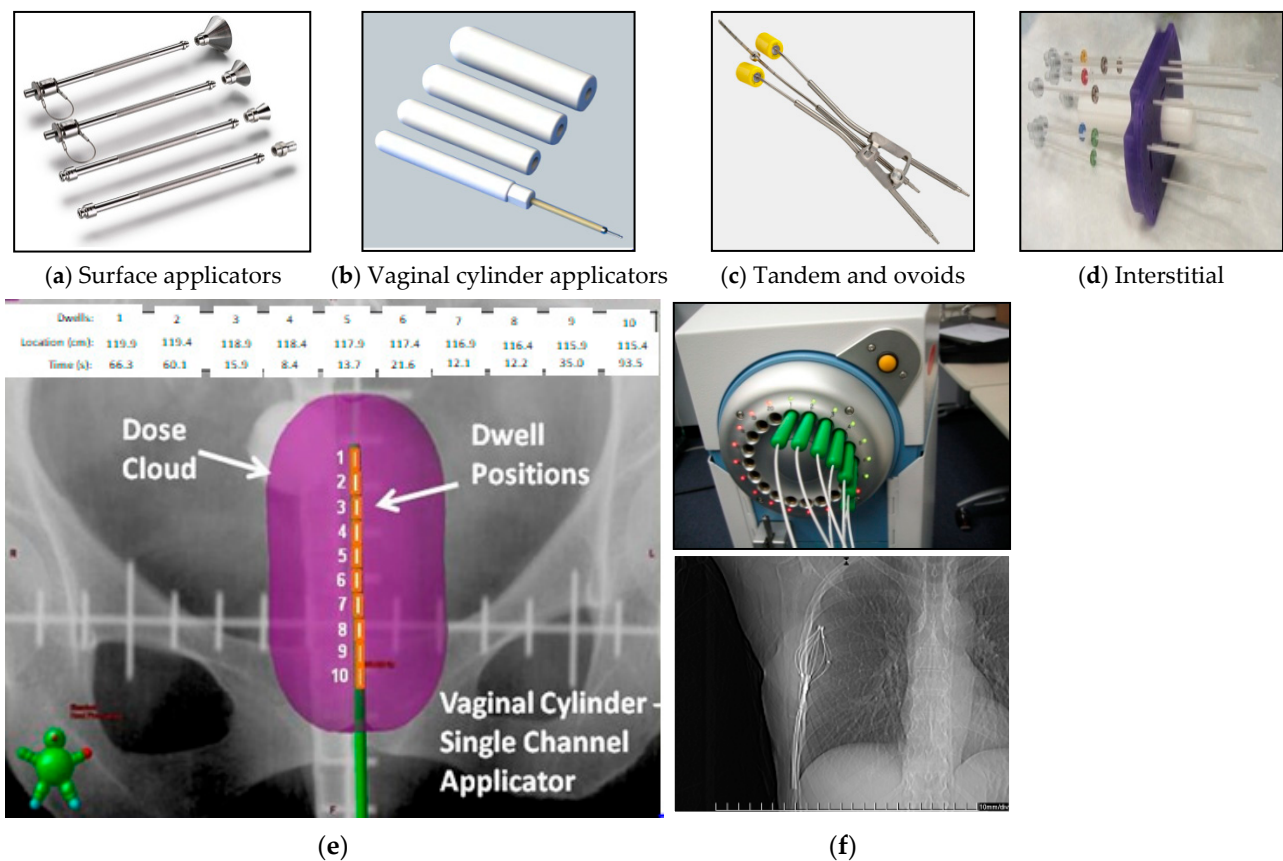


Figure 3. Surface applicators for skin cancer treatments (a), cylindrical applicators for vaginal and rectal cancer treatments (b), tandem and ovoids (Fletcher Suit) for cervical and uterine cancer treatments (c), interstitial needle array for interstitial gynecological or prostate treatments (d), number of dwells (1–10), dwell positions (locations in cm), dwell times (s), and dose distributions for a brachytherapy treatment using a cylindrical applicator [33]. (e). SAVI applicator catheters connected to a ¹⁹²Ir HDR source (f-top) and coronal radiograph of the SAVI applicator inside a patient (f-bottom).

The computer simulation provides a calculated dose distribution in three dimensions (3D) that can be adjusted by increasing/decreasing dwell times for optimal dose conformity to the tumor volume and minimal collateral dose elsewhere. The final dose is calculated by summing the dose contribution from each dwell position in each applicator channel.

A similar process could be used with an LWFA-HDR system. A catheter connected to an applicator is replaced by a fiber-optic channel where a laser beam could travel and irradiate a nano-particle cavity to produce an electron beam that can be emitted from the channel’s tip. A computer simulation performed prior to treatment could determine the appropriate electron beam energy or mixed energies (for greater treatment depth), beam directionality, optimal dose distribution to the target volume, and collateral dose to healthy organs nearby. Further, a new LWFA-HDR applicator could be made of material to minimize electron beam attenuation and facilitate fiber-optic channel connectivity for treatment delivery.

The simplest clinical application of an LWFA-HDR could be in the treatment of skin cancers [34–38]. At present, 50 kV X-ray beams from electronic generators (e.g., Xofigo Axxent, iCAD Inc., San Jose, CA, USA) and 6–12 MeV linac-based electron beams (e.g., Mobetron, IntraOp Medical Corporation, Sunnyvale, CA, USA), in addition to conventional HDR brachytherapy, are available for skin cancer treatment. From these technologies, only the 50 kV X-ray generator for electronic brachytherapy is portable, and one energy is available. An LWFA-HDR system could offer portability and a selection of electron beam energies suitable for superficial and deep-seated skin cancers. Moreover, electron beams emitted

from fiber-optic channel tips could facilitate treating skin cancers near or at the nasal ridge, eyes, and ears, to name a few, where irregular anatomical surfaces are encountered.

In addition to comparable capabilities to current HDR systems, an LWFA-HDR could be used in theranostic and intraoperative radiation therapy (IORT). For instance, some liver cancers are treated with radioembolization, which involves injecting a radioactive solution containing ^{90}Y into the cancer(s) through its (their) blood supply. Perhaps, rather than using a radioactive solution for treatment, the LWFA-HDR could be used instead. A specially-designed fiber-optic channel(s) with a miniature camera for endoscopy and for LWFA electron beam irradiation could be sent to the liver cancer through the femoral artery near the groin. Real-time imaging of the treatment site could be used to aim the electron beam (or beams) and deliver a radiation dose. The development of a miniature endoscope that can travel through a blood vessel and provide essential imaging is in progress and could be available in the near future [39]. Hence, LWFA-HDR could provide a theranostic capability that, at present, is not available in radiation therapy.

Furthermore, the LWFA-HDR theranostic capability combined with vector-medicine, which identifies and tags cancer cells [40,41], could be a high-precision treatment against cancer. High-Z materials such as gadolinium and iodine could be attached to vector molecules. These molecules seek and bind to cancer cells identifying them as targets that, subsequently, could be aimed with the LWFA-HDR electron beam(s). In this way, the electron beam(s) aims not only to rely on real-time endoscopic imaging but also on specific cell biomarkers. Such biomarking can enhance treatment accuracy and reduce collateral damage.

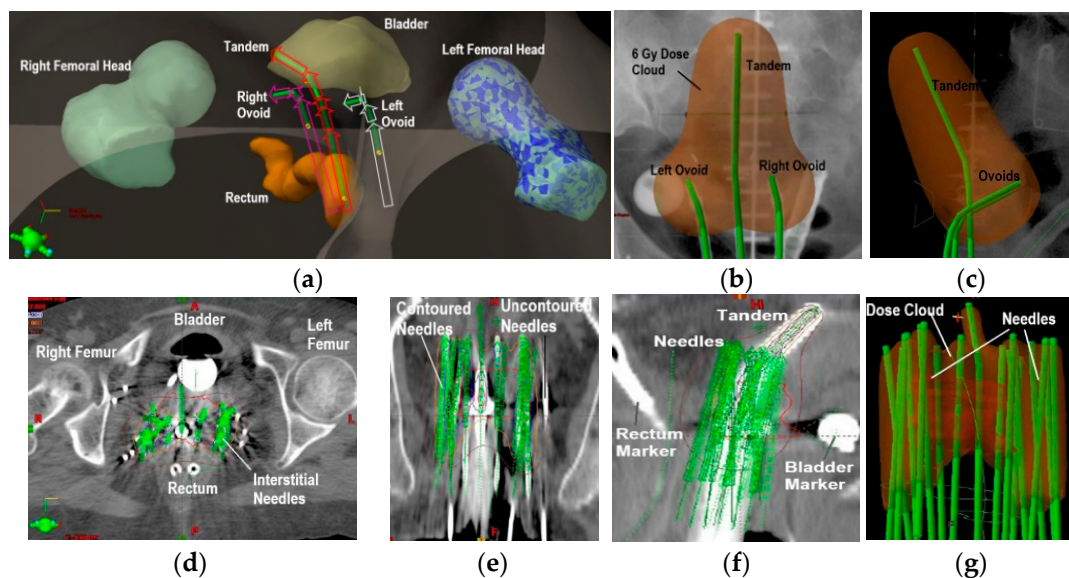


Figure 4. Three-dimensional computer rendering of a tandem-and-ovoids brachytherapy treatment generated from a patient's CT scan. Femoral heads, bladder, and rectum structures are depicted. The arrows in the green structures indicate the radiation treatment is administered with the source at the most distal dwell position (or farthest inside the applicator) first per applicator channel (a). A calculated 6 Gy prescription dose distribution (pear shape) for a tandem-and-ovoids (green structures) is shown in a coronal (b) and sagittal views (c). Axial CT image depicting interstitial brachytherapy needles for cervical cancer treatment (d). Coronal (e) and sagittal images (f) are also shown. Depiction of a 6 Gy prescription dose calculated from the dose contribution of all the interstitial needle channels (g).

3.3. Potential for FLASH Brachytherapy

FLASH is a proposed treatment modality under investigation for external beam radiotherapy (not brachytherapy) that is gaining interest in radiation oncology [42]. The significant difference between FLASH and conventional radiotherapy is the dose rate

used. FLASH dose rate ranges from 50–400 Gy/s compared to 0.1–0.4 Gy/s for standard treatments. Ongoing radiobiological studies suggest that, at these dose rates, FLASH can spare healthy tissues by depleting them from their oxygen content and making them radioresistant. Further, it is theorized that FLASH could take advantage of a tumor’s iron content, which is higher than healthy tissues, to inflict lethal damage to malignant cells and trigger apoptosis [42]. However, more basic (laboratory/animal) research and technology development (e.g., new linacs with FLASH dose rates) followed by human clinical trials remains to be done to fully elucidate a FLASH treatment capability [42,43].

Most of the hardware development for FLASH has been focused on external beam radiotherapy and not on brachytherapy delivery systems. Although work has been done in the production of sub-MeV LWFA electrons with ultrahigh instantaneous dose rates (~10 Gy/s), the average dose is still below what is required for FLASH [44]. It could be speculated that a sufficiently powerful laser source irradiating an optimized plasma/nanoparticle medium could produce electron beams with dose rates that approximate FLASH. If that is possible, LWFA-HDR brachytherapy could be further revolutionized with this enhanced capability.

4. Cost Benefits and Market Size

As previously mentioned, minimal radiation shielding would be required to operate an LWFA-HDR system which can lead to significant savings for radiation oncology clinics due to a reduction in construction and shielding material costs. Any room could be easily retrofitted for treatment at a fraction of the price of an existing HDR treatment room. Moreover, it would eliminate the replacement and purchase of new radioactive sources due to source decay every 4–6 months for ¹⁹²Ir and 2–3 years for ⁶⁰Co, which results in further savings for the clinic.

It is expected that radiation oncology centers may be enticed to replace their existing HDR units with an LWFA-HDR system, primarily for the cost savings that it would provide. Moreover, not using a radioactive source in brachytherapy treatments eliminates the security risks that a source implies, which could be further persuasive reasons for adopting this technology. Table 1 provides a cost estimate comparison between existing HDR units and the proposed LWFA-HDR system. The estimated cost for an LWFA-HDR system accounts for laser source, and fiber-optic channel setup (see Figure 2) costs [22,44]. Costs for ¹⁹²Ir and ⁶⁰Co HDR units, room shielding construction, and source replacement are based on current market prices [45–48].

Table 1. Estimated purchase and maintenance cost comparisons for LWFA-HDR and conventional HDR systems.

Item	LWFA-HDR	¹⁹² Ir-HDR	⁶⁰ Co-HDR
Purchase Estimate (one-time expense)	\$100K–\$300K	\$200K–\$350K	~\$300K
Room Shielding (one-time expense)	None	\$200K–\$500K *	\$300K–\$500K **
Source Replacement	None	~\$10K every 4–6 months	~130K every 60 months
Downtime due to Source Replacement	None	1–2 days	1–2 days
5-year Estimated Total	\$300K	\$910K	\$930K

* US cost estimates [46,47]. ** Latin America cost estimates [48].

Table 2 provides information on radiotherapy linacs available worldwide in 2013 according to the 2015 Lancet Oncology Commission report [49], and Table 3 shows the number of radiotherapy linacs that were available in the United States in 2004 [50]. Although this number may be greater in 2022, the 2004 data was used to provide a conservative market size illustration for a LWFA-HDR system.

Table 2. Total number of radiotherapy linacs that were available worldwide in 2015 and reported in Lancet stratified by high, upper-middle, and low-income countries.

HI	UMI	LMI	LI	Total
8911 (68%)	3115 (24%)	1014 (8%)	32 (0%)	13,072 (100%)

HI = High-Income countries; UMI = Upper-Middle-Income countries; LMI = Lower-Middle-Income countries; LI = Low-Income countries.

Table 3. Radiation oncology clinics and radiotherapy linacs were available in the United States in 2004.

Rad. Onc. Clinics in the US in 2004	Radiotherapy Linacs
2246	5166

On average, the number of available HDR brachytherapy units in HI and UMI countries is ~20% of the number of radiotherapy linacs [51]. Therefore, from Table 2, these correspond to 1782 and 623 HDR units in HI and UMI countries, respectively. No published data was found on HDR units in LMI and LI countries. Based on this information and assuming a \$300K cost (see Table 1) for an LWFA-HDR unit, the total addressable market (TAM) revenue estimate from HI and UMI countries could be \$722M. Narrowing the market to HI countries, the serviceable available market (SAM) revenue estimate reduces to \$534M. For the US market and using the data in Table 3, 1033 HDR units were available in the US in 2004. Therefore, the serviceable obtainable market (SOM) revenue estimate in the US market could be \$310M. Figure 5 provides a market size depiction for the LWFA-HDR system.

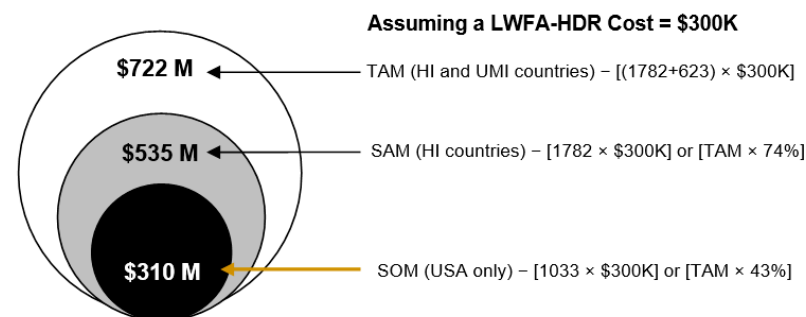


Figure 5. Estimated revenue from the LWFA-HDR brachytherapy system in HI & UMI, HI only, and US (based on Table 2 data) markets. Market size is depicted in terms of the total addressable market (TAM), serviceable available market (SAM), and serviceable obtainable market (SOM).

As indicated, this analysis does not include potential revenue from LMI and LI countries. However, it can be speculated that this technology could be of significant interest to those regions and, likely, within their financial means to afford it.

5. Conclusions

The aim of this paper was to present a vision of what could be achievable with electron beams produced via LWFA and their use in cancer treatments with brachytherapy. Furthermore, to describe the cost savings that an LWFA-HDR system could provide to a radiation oncology clinic since it eliminates the use of radioactive sources and radiation-shielded rooms for treatment. Although an in-depth analysis of the LWFA electron beam dosimetry applied to brachytherapy is not included, it will be forthcoming as the technology develops further.

An LWFA-HDR system with its capabilities described in this paper could significantly transform the delivery of brachytherapy treatments while making them more accessible and cost-effective to radiation oncology clinics, particularly in low- to middle-income countries.

Funding: This research received no external funding.

Institutional Review Board Statement: Not applicable.

Informed Consent Statement: Not applicable.

Data Availability Statement: Not applicable.

Acknowledgments: We are much indebted to Donna Strickland, W. J. Sha, J-C. Chanteloup for the fiber laser technology. We are grateful for discussions on LWFA with nano-materials with E. Barraza-Valdez, S. Nicks.

Conflicts of Interest: The authors declare no conflict of interest.

References

1. Tajima, T.; Dawson, J.M. Laser electron accelerator. *Phys. Rev. Lett.* **1979**, *43*, 267–270. [[CrossRef](#)]
2. Strickland, D.; Mourou, G. Compression of amplified chirped optical pulses. *Opt. Comm.* **1985**, *56*, 219–221. [[CrossRef](#)]
3. Nakajima, K.; Nakanishi, H.; Kawakubo, T.; Ogata, A.; Kitagawa, Y.; Shiraga, H.; Zhang, T.; Suzuki, K.; Kato, Y.; Sakawa, Y.; et al. Laser wakefield accelerator experiments using 1ps 30 TW Nd:glass laser. In Proceedings of the International Conference on Particle Accelerators, Washington, DC, USA, 17–20 May 1993; IEEE: Piscataway, NJ, USA, 1993; pp. 2556–2558.
4. Modena, A.; Najmudin, Z.; Dangor, A.E.; Clayton, C.E.; Marsh, K.A.; Joshi, C.; Malka, V.; Darrow, C.B.; Danson, C.; Neely, D.; et al. Electron acceleration from the breaking of relativistic plasma waves. *Nature* **1995**, *377*, 606–608. [[CrossRef](#)]
5. Mangles, S.P.D.; Murphy, C.D.; Najmudin, Z.; Thomas, A.G.R.; Collier, J.L.; Dangor, A.E.; Divall, E.J.; Foster, P.S.; Gallacher, J.G.; Hooker, C.J.; et al. Monoenergetic beams of relativistic electrons from intense laser-plasma interactions. *Nature* **2004**, *431*, 535–538. [[CrossRef](#)] [[PubMed](#)]
6. Geddes, C.G.R.; Toth, C.S.; van Tilborg, J.; Esarey, E.; Schroeder, C.B.; Bruhwiler, D.; Nieter, C.; Cary, J.; Leemans, W.P. High-quality electron beams from a laser wakefield accelerator using plasma-channel guiding. *Nature* **2004**, *431*, 538–541. [[CrossRef](#)] [[PubMed](#)]
7. Faure, J.; Glinec, Y.; Pukhov, A.; Kiselev, S.; Gordienko, S.; Lefebvre, E.; Rousseau, J.P.; Burgy, F.; Malka, V. A laser-plasma accelerator producing monoenergetic electron beams. *Nature* **2004**, *431*, 541–544. [[CrossRef](#)] [[PubMed](#)]
8. Leemans, W.P.; Nagler, B.; Gonsalves, A.J.; Toth, C.S.; Nakamura, K.; Geddes, C.G.R.; Esarey, E.; Schroeder, C.B.; Hooker, S.M. GeV electron beams from a centimetre-scale accelerator. *Nat. Phys.* **2006**, *2*, 696–699. [[CrossRef](#)]
9. Hafz, N.A.M.; Jeong, T.M.; Choi, I.W.; Lee, S.K.; Pae, K.H.; Kulagin, V.V.; Sung, J.H.; Yu, T.J.; Hong, K.-H.; Hosokai, T.; et al. Stable generation of GeV-class electron beams from self-guided laser-plasmas channels. *Nat. Photonics* **2008**, *2*, 571–577. [[CrossRef](#)]
10. Gonsalves, A.J.; Nakamura, K.; Daniels, J.; Benedetti, C.; Pieronek, C.; de Raadt, T.C.H.; Steinke, S.; Bin, J.H.; Bulanov, S.S.; van Tilborg, J.; et al. Petawatt Laser Guiding and Electron Beam Acceleration to 8 GeV in a Laser-Heated Capillary Discharge Waveguide. *Phys. Rev. Lett.* **2019**, *122*, 084801. [[CrossRef](#)]
11. Giulietti, A.; Bourgeois, N.; Ceccotti, T.; Davoine, X.; Dobosz, S.; Oliveira, P.D.; Galimberti, M.; Galy, J.; Gamucci, A.; Giulietti, D.; et al. Intense g-ray source in the giant-dipole-resonance range driven by 10-TW laser pulses. *Phys. Rev. Lett.* **2008**, *101*, 105002. [[CrossRef](#)]
12. Nakajima, K.; Yuan, J.; Chen, L.; Sheng, Z. Laser-driven very high energy electron/photon beam radiation therapy in conjunction with a robotic system. *Appl. Sci.* **2015**, *5*, 1–20. [[CrossRef](#)]
13. Nakajima, K. Laser-driven electron beam and radiation sources for basic, medical and industrial sciences. *Proc. Jpn. Acad. Ser. B* **2015**, *91*, 223–245. [[CrossRef](#)] [[PubMed](#)]
14. Giulietti, A. *Laser-Driven Particle Acceleration towards Radiobiology and Medicine*; Biological and Medical Physics, Biomedical Engineering; Springer: Berlin, Germany, 2016; ISSN 2197-5647.
15. Fourkal, E.; Shahine, B.; Ding, M.; Li, J.S.; Tajima, T.; Ma, C.M. Particle in cell simulation of laser-accelerated proton beams for radiation therapy. *Med. Phys.* **2002**, *29*, 2788–2798. [[CrossRef](#)] [[PubMed](#)]
16. Fourkal, E.; Li, J.S.; Ding, M.; Tajima, T.; Ma, C.M. Particle selection for laser-accelerated proton therapy feasibility study. *Med. Phys.* **2003**, *30*, 1660–1670. [[CrossRef](#)]
17. Macchi, A. A review of laser-plasma ion acceleration. *arXiv* **2017**, arXiv:1712.06443v1.
18. Nicks, B.S.; Hakimi, S.; Barraza-Valdez, E.; Chesnut, K.D.; DeGrandchamp, G.H.; Gage, K.R.; Housley, D.B.; Huxtable, G.; Lawler, G.; Lin, D.J.; et al. Electron dynamics in the high-density laser-wakefield acceleration regime. *Photonics* **2021**, *8*, 216. [[CrossRef](#)]
19. Barraza-Valdez, E.; Tajima, T.; Strickland, D.; Roa, D. Laser beat wave acceleration near critical density. *Photonics* **2022**. *submitted*.
20. National Cancer Institute—Radiation Therapy to Treat Cancer. Available online: <https://www.cancer.gov/aboutcancer/treatment/types/radiation-therapy/brachytherapy> (accessed on 25 March 2022).
21. Khan, F.M. *The Physics of Radiation Therapy*, 4th ed.; Lippincott Williams & Wilkins: New York, NY, USA, 2010.
22. Shah, W.; Chanteloup, J.C.; Mourou, G. Ultrafast fiber technologies for compact laser wake-field in medical applications. *Photonics* **2022**. *submitted*.
23. Renner, W.D.; O'Connor, T.P.; Bermudez, N.M. An algorithm for generation of implant plans for high-dose-rate irradiators. *Med. Phys.* **1990**, *17*, 35–40. [[CrossRef](#)]

24. Arnold, C.A.; Pezhohou, M.K.; Lam-Himlin, D.; Pittman, M.E.; VandenBussche, C.; Voltaggio, L. 90Y-TheraSpheres: The new look of Yttrium-90. *Am. J. Surg. Pathol.* **2019**, *43*, 688–694. [CrossRef]
25. Salem, R.; Lewandowski, R.J.; Mulcahy, M.F.; Riaz, A.; Ryu, R.K.; Ibrahim, S.; Atassi, B.; Baker, T.; Gates, V.; Miller, F.H.; et al. Radioembolization for Hepatocellular Carcinoma Using Yttrium-90 Microspheres: A Comprehensive Report of Long-term Outcomes. *Gastroenterology* **2010**, *138*, 52–64. [CrossRef] [PubMed]
26. Salem, R.; Johnson, G.E.; Kim, E.; Riaz, A.; Bishay, V.; Boucher, E.; Fowers, K.; Lewandowski, R.; Padia, S.A. Yttrium-90 Radioembolization for the treatment of solitary, unresectable HCC: The legacy study. *Hepatology* **2021**, *74*, 2342–2352. [CrossRef] [PubMed]
27. Kennedy, A.S.; Coldwell, D.; Nutting, C.; Murthy, R.; Wertman, D.E., Jr.; Loehr, S.P.; Overton, C.; Meranze, S.; Niedzwiecki, J.; Sailer, S. 90Y-microsphere brachytherapy for unresectable colorectal liver metastases: Modern USA experience. *Int. J. Radiat. Oncol. Biol. Phys.* **2006**, *65*, 412. [CrossRef] [PubMed]
28. Van der Laars, R.; Prius, T.P.E. Introduction to HDR brachytherapy optimization. In *Brachytherapy from Radium to Optimization*; Nucletron Corporation: Veenendaal, The Netherlands, 1994.
29. Ezzel, G.A.; Luthermann, R.W. Clinical implementation of dwell time optimization techniques for single stepping-source remote applicators. In *Brachytherapy Physics*; Medical Physics Publishing: Madison, WI, USA, 1994.
30. Kubo, H.D.; Glasgow, G.P.; Pethel, T.D.; Thomadsen, B.R.; Williamson, J.F. High dose-rate brachytherapy treatment delivery: Report of the AAPM Radiation Therapy Committee Task Group No. 59. *Med Phys.* **1998**, *25*, 375–403. [CrossRef]
31. Ramachandran, P. New era of electronic brachytherapy. *World J. Radiol.* **2017**, *9*, 148–154. [CrossRef]
32. Valentin, J. Preface, Main Points, Introduction, Chapters 2 and 3. *Ann. ICRP* **2005**, *35*, 1–9. [CrossRef]
33. IAEA. 3D Brachytherapy Treatment Planning. Available online: https://inis.iaea.org/collection/NCLCollectionStore/_Public/49/093/49093364.pdf (accessed on 25 March 2022).
34. IAEA. *The Transition from 2-D Brachytherapy to 3-D High Dose Rate Brachytherapy*; Human Health Report No. 12.; IAEA: Vienna, Austria, 2015.
35. Chua, B.; Jackson, J.E.; Lin, C.; Veness, M.J. Radiotherapy for early non-melanoma skin cancer. *Oral Oncol.* **2019**, *98*, 96–101. [CrossRef]
36. Garbutcheon-Singh, K.B.; Veness, M.J. The role of radiotherapy in the management of non-melanoma skin cancer. *Australas. J. Dermatol.* **2019**, *60*, 265–272. [CrossRef]
37. Ota, K.; Adar, T.; Dover, L.; Khachemoune, A. Review: The reemergence of brachytherapy as treatment for non-melanoma skin cancer. *J. Dermatol. Treat.* **2018**, *29*, 170–175. [CrossRef]
38. Veness, M.; Delishaj, D.; Barnes, E.; Bezugly, A.; Rembielak, A. Current Role of Radiotherapy in Non-melanoma Skin Cancer. *Clin. Oncol.* **2019**, *31*, 749–758. [CrossRef]
39. Li, J.; Thiele, S.; Quirk, B.C.; Kirk, R.W.; Verjans, J.W.; Akers, E.; Bursill, C.A.; Nicholls, S.J.; Herkommer, A.M.; Giessen, H.; et al. Ultrathin monolithic 3D printed optical coherence tomography endoscopy for preclinical and clinical use. *Light Sci. Appl.* **2020**, *9*, 124. [CrossRef] [PubMed]
40. Matsumoto, K.; Saitoh, H.; Doan, T.L.H.; Shiro, A.; Nakai, K.; Komatsu, A.; Tsujimoto, M.; Yasuda, R.; Kawachi, T.; Tajima, T.; et al. Destruction of tumor mass by gadolinium-loaded nanoparticles irradiated with monochromatic X-rays: Implications for the Auger therapy. *Sci. Rep.* **2019**, *9*, 13275. [CrossRef] [PubMed]
41. Higashi, Y.; Matsumoto, K.; Saitoh, H.; Shiro, A.; Ma, Y.; Laird, M.; Chinnathambi, S.; Birault, A.; Doan, T.L.H.; Yasuda, R.; et al. Iodine containing porous organosilica nanoparticles trigger destruction of tumor spheroids upon irradiation with monochromatic X-ray: DNA double strand breaks and preferential effect of K-edge energy X-ray. *Sci. Rep.* **2021**, *11*, 14192. [CrossRef] [PubMed]
42. Wilson, J.D.; Hammond, E.M.; Higgins, G.S.; Petersson, K. Ultra-High dose rate (FLASH) radiotherapy: Silver bullet or fool's gold? *Front. Oncol.* **2020**, *9*, 1563. [CrossRef]
43. Ashraf, M.R.; Rahman, M.; Zhang, R.; Williams, B.B.; Gladstone, D.J.; Pogue, B.W.; Bruza, P. Dosimetry for FLASH Radiotherapy: A Review of Tools and the Role of Radioluminescence and Cherenkov Emission. *Front. Phys.* **2020**, *8*, 328. [CrossRef]
44. Labate, L.; Andreassi, M.G.; Baffigi, F.; Bizzarri, R.; Borghini, A.; Bussolino, G.C.; Fulgentini, L.; Ghetti, F.; Giulietti, A.; Koster, P. LESM: A laser driven sub-MeV electron source delivering ultra-high dose rate on thin biological samples. *J. Appl. Phys. D Appl. Phys.* **2016**, *49*, 275401. [CrossRef]
45. Sha, W.; CommScope Access Technologies Advanced Research, Santa Clara, CA, USA. Private communication, 2022.
46. Varian Medical Systems Sales Representative; Varian Medical Systems, Palo Alto, CA, USA. Private communication, 2022.
47. Scanderbeg, D.J.; Yashar, C.; Ouhib, Z.; Jhingran, A.; Einck, J. Development, implementation and associated challenges of a new HDR brachytherapy program. *Brachytherapy* **2020**, *19*, 874–880. [CrossRef]
48. Mailhot Vega, R.B.; Barbee, D.; Talcott, W.; Duckworth, T.; Shah, B.A.; Ishaq, O.F.; Small, C.; Yeung, A.R.; Perez, C.A.; Schiff, P.B.; et al. Cost in perspective: Direct assessment of American market acceptability of Co-60 in gynecologic high-dose-rate brachytherapy and contrast with experience abroad. *J. Contemp. Brachyther.* **2018**, *10*, 503–509. [CrossRef]
49. Atun, R.; Jaffray, D.A.; Barton, M.B.; Bray, F.; Baumann, M.; Vikram, B.; Hanna, T.P.; Knaul, F.M.; Lievens, Y.; Lui, T.Y.; et al. Expanding global access to radiotherapy. *Lancet* **2015**, *16*, 1153–1186. [CrossRef]
50. Ballas, L.K.; Elkin, E.B.; Schrag, D.; Minsky, B.D.; Bach, P.B. Radiation therapy facilities in the United States. *Int. J. Radiat. Oncol. Biol. Phys.* **2006**, *66*, 1204–1211. [CrossRef] [PubMed]
51. IROC; University of Texas—MD Anderson Cancer Center, Houston, TX, USA. Private communication, 2022.